Journal of Physical and Theoretical Chemistry
of Islamic Azad University of Iran, 14 (3) 211-228: Fall 2017
(J. Phys. Theor. Chem. IAU Iran)
ISSN 1735-2126

A computational study of Nitramide adsorption on the surface of pristine and Ni functionalized (4,4) armchair Gallium nitride nanotubes

M. Rezaei−Sameti* and S. Baranipour

Department of Applied Chemistry, Faculty of Science, Malayer University, Malayer, 65174, Iran

Received December 2017; Accepted February 2018

ABSTRACT

By using the density function theory (DFT) the adsorption of nitramine (NH_2NO_2) molecule on the surface of pristine and Ni functionalized of Gallium nitride nanotube (GaNNTs) is investigated. The adsorption energy of NH_2NO_2 molecule on the surface of pristine and Ni functionalized GaNNTs is in range −6.59 to −48.16 Kcal/mol and is physisorption type. The ΔE and ΔH values of the all adsorption models are in range −10.34 to −47.17 Kcal/mol and −13.43 to −47.77 Kcal/mol respectively, the negative values of ΔE and ΔH reveal that the adsorption of NH_2NO_2 molecule on the surface of pristine and Ni functionalized GaNNTs is exothermic. The molecular electronic potential (MEP) indicates that a low electron charge is transferred from the NH_2NO_2 molecule toward the nanotube ones resulting in the exterior surface of nanotube is rich of electron charge. The HOMO energy of adsorbed models on the pristine GaNNTs is lower than Ni functionalized.

Keywords: NH_2NO_2 adsorption; GaNNTs; Ni−functionalized; Density function theory; Molecular electrostatic potential

1. INTRODUCTION

Recent advances in the fabrication and procurement of carbon nanotubes cause that the extensive research activities on structural, electrical, optical, magnetic, mechanical properties and their potential applications in nanoelectronic, nanolithography, photocatalysis, microscopy, and other fields of nanomaterial have also been investigated [1, 2].

Among of the nanotubes and nanoparticles in the third and fifth groups' periodic table, the gallium nitride has been of great interest to researchers due to its low dimensionality, quantum size, and unique electrical and optoelectronic properties [3–7].

GaNNTs, similar carbon and boron nitride nanotube, is expected to be capable of forming interesting allotropes. For this purpose, at the recent year many studies have been done to synthesize and formation of various nanotube, nanowires, amorphous and single crystal of gallium nitride with different methods [8−12].

Due to unique structural, electrical, mechanical and optoelectronic properties of GaN nanotube, many theoretical and experimental researches have been done [13−17]. The results of these researches

*Corresponding author: mrsameti@gmail.com, mrsameti@malayeru.ac.ir

confirm that the band gap of Wurtzite phase of GaN is close to 3.4 eV and it can be used as a possible material storage medium, adsorbent of metals, gas and other environmental toxic materials and various applications in devices such as electronic, radiation resistant detectors, laser diodes, and the electromechanical [18−27].

In the recent years the progress of the industry has led to a dramatic increase the toxic and pollution materials in the nature. These harmful substances affect the health of humans and other living organisms. One of these harmful compounds is Nitramine. Nitroamine (NH_2NO_2) is the simplest prototype of nitramine energetic materials and organic nitrate explosives [28−29]. The interaction of nitroamine with various nanoparticles such as Al clusters, Al_2O_3(0 0 1) and Al(111) showed that the NH_2NO_2 dissociate to O atom(s) and NH_2NO or NH_2N species [30−35]. In previous work, the effects of NH_2NO_2 adsorption and interaction on the surface of pristine and C−replaced boron nitride nanosheet is investigated [34]. In the current work we survey the effects of NH_2NO_2 adsorption and interaction on the surface of pristine and Ni functionalized GaNNTs by using cam−B3LYP/6−31G(d) level of theory. For this means the thermodynamic parameters, HOMO−LUMO and electrical properties, Natural bond orbital (NBO) analysis and Molecular electronic potential plots (MEP) for all considered models are calculated and results for all models are analyzed.

2. COMPUTATIONAL DETAILS

All calculations are performed with the GAMESS suite of programs by using DFT method at cam−B3LYP level of theory using the 6−31G (d) base set [36]. For investigating the effects of orientation NH_2NO_2 adsorption on the surface of pristine and Ni functionalized GaNNTs, we examine different configurations of NH_2NO_2 on the surface of nanotube. All considered configuration structures are optimized by using B3LYP/3−21G level of computational method to check the the lowest−energy, equilibrium geometries and electronic properties for the adsorbate/adsorbent system. After optimizing all considered configurations, we select the sixteen suitable configurations without imaginary frequencies. The selected configurations of NH_2NO_2 molecule on the surface of pristine and Ni functionalized GaNNTs are full optimized again by using cam−B3LYP/6−31G (d) level of theory. In Fig. 1 the adsorption positions of NH_2NO_2 molecule on the surface of nanotube are denoted by a, b, c and d. To specify 16 absorbing models, we use A, B, C and D label.

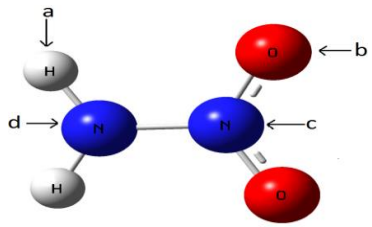

Fig. 1. 2D views of position of NH_2NO_2 adsorption gas on the surface of pristine and Ni functionalized GaNNTs.

The A and B labels are used for adsorbing NH_2NO_2 on the Ga and N site of pristine nanotube respectively. The C and D labels are applied for adsorbing NH_2NO_2 on the Ni site and backside of Ni functionalized nanotube (see Fig. 2).

To reduce the calculation time, length of nanotube and dangling effects the ends of all nanotube are saturated by hydrogen atom. The thermodynamic parameters, adsorption energy, quantum parameters, NBO results, MEP plots, and density of state (DOS) plots of all studied models are calculated and results are analyzed.

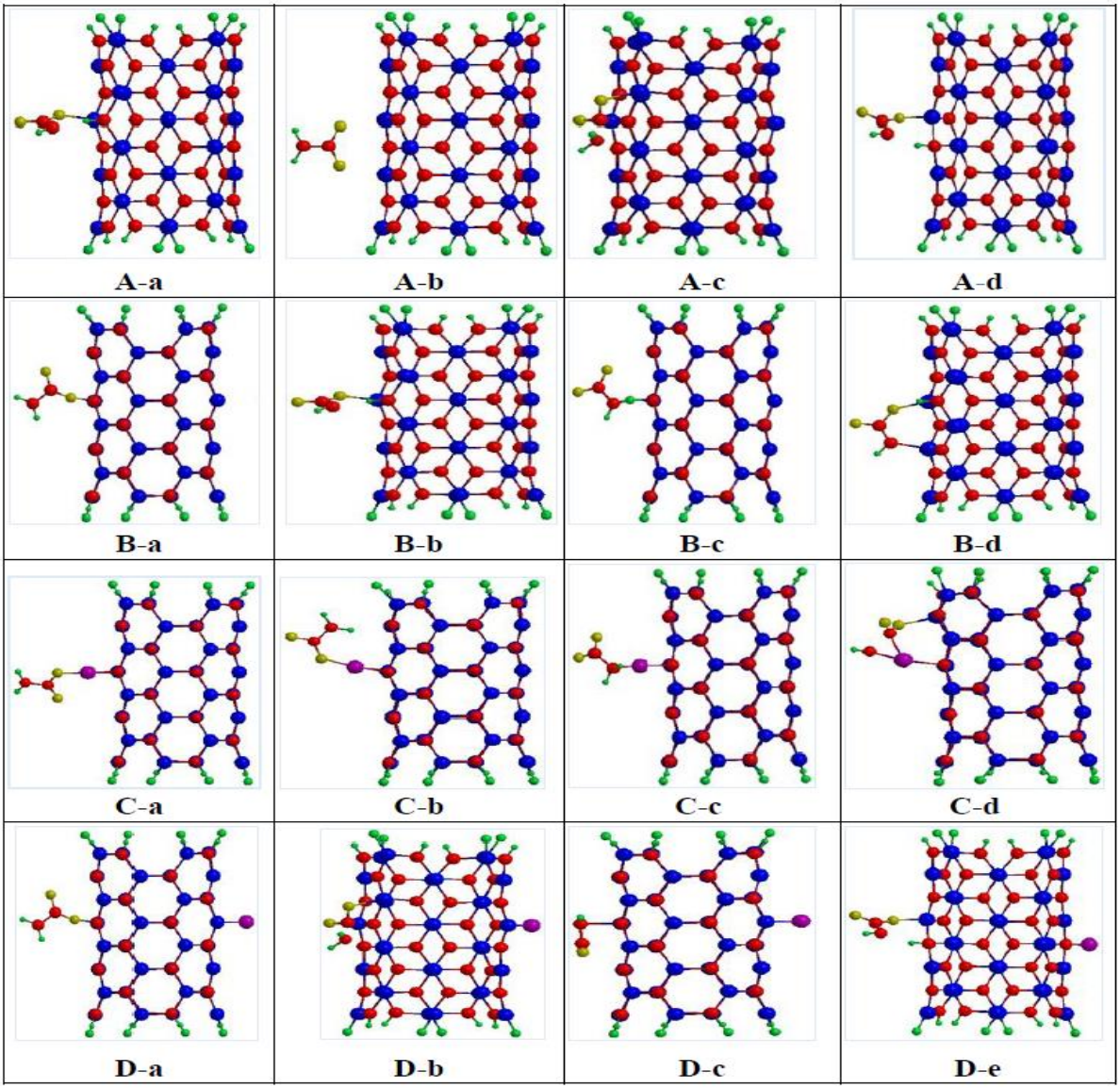

Fig. 2. 2D views of NH_2NO_2 adsorption gas on the surface of pristine and Ni functionalized GaNNTs at A−a to D−d models.

3. RESULTS AND DISCUSSION

3.1 Structural parameters

The optimized structures of the A−a to D−d adsorption models are displayed in Fig. 2. The calculated average Ga−N bond lengths around adsorption position in A, B, C and D models are about 1.85, 1.87, 1.87, 1.88 Å respectively (see Fig. 3) and these results are in agreement with other reported results [31−33]. The average Ga−N−Ga bond angels of A, B, C and D are about 120º, 119º, 120º and 118º respectively.

A comparison result demonstrates that with functionalizing Ni atom and adsorbing NH_2NO_2 the bond length and bond angel of GaNNTs alter slightly from pristine and unabsorbed state. The dipole moment (μ_d) values for all adsorption models are in range 4.05 to 9.10 debay. Whereas the bond distance between NH_2NO_2 molecule and nanotube is in

range 1.04 to 4.04 Å. The most bond distance have been seen in the C−b model with dipole moment 7.60 debay, and the lowest bond distance is found in the A−a and A−b models with dipole moment 5.99 Å. In other to investigate the interaction behavior between NH_2NO_2 with GaNNTs, we calculate the adsorption energy (E_{ads}) of all studied models by using Eq. 1:

$$E_{ads} = E_{NH2NO2/nanotube} - (E_{NH2NO2} + E_{nanotube}) + BSSE \quad (1)$$

Here $E_{NH2NO2/nanotube}$, E_{NH2NO2} and $E_{nanotube}$ are the optimized potential energies of NH_2NO_2/nanotube, NH_2NO_2 and nanotube respectively. The calculated base set superposition error (BSSE) values for all adsorption is in range 0.0005 to 0.001.

Based on the calculated results in Table 1, the NH_2NO_2 molecule can be absorbed on the surface pristine and Ni functionalized GaNNTs physically with the adsorption (E_{ads}) in range −6.59 to −48.16 Kcal/mol. In all adsorption models except C−d model the adsorption energy of H (NH_2) site of NH_2NO_2 on the surface of nanotube (A−a, B−a, C−a and D−a models) is more favorable than other models. Model C−d with the highest absorption energy (−48.16 Kcal/mol) is the most favorable model for absorbing Nitramine on a GaN nanotube. When the NH_2NO_2 molecules close from O site over surface of nanotube except C−b model the adsorption of NH_2NO_2/nanotube complex is significantly lower than H site. Therefore, the adsorption and interaction of NH_2NO_2 molecule from H site is more favorable than O site. The adsorption energy of N (NH2) in d orientation for A−d, B−d, C−d and D−d models are −34.03, −6.59, −48.16 and −35.37 Kcal/mole respectively.

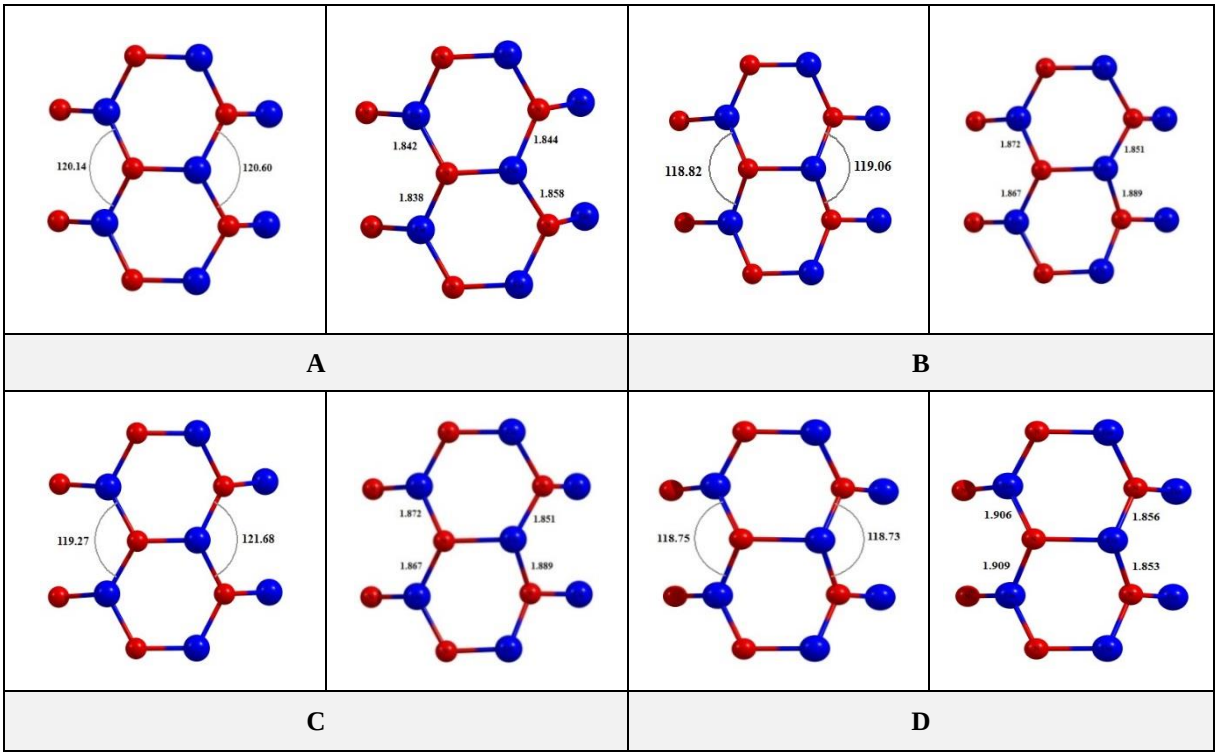

Fig. 3. Plots of bond length and bond angel for A−a to D−d adsorption models (see Fig. 2).

Table 1. Calculated adsorption, deformation energy of nanotube, NH_2NO_2, binding energy (E_{int}) (Kcal. mol^{-1}) for A-a to D-d models (see Figs. 1-4).

Properties	A - a	A – b	A - c	A - d	B-a	B-b	B-c	B-d
E_{ads}	-37.27	-10.53	-28.02	-34.03	-37.64	-10.01	-14.03	-6.59
$E_{def\ NH2NO2}$	-110.96	-0.83	-60.35	-115.01	-2.11	-0.63	-0.46	-60.44
$E_{def\ nano}$	-21.83	-3.42	-29.62	-21.18	-22.73	-2.48	-3.56	-31.31
$E_{def\ tot}$	-132.79	-4.26	-89.97	-136.19	-134.45	-3.31	-4.02	-91.75
E_{bin}	-170.06	-14.78	-117.99	-170.22	-179.09	-14.43	-18.05	-118.35
d	1.05	1.05	2.39	2.17	3.27	3.76	1.93	3.37
$\Delta\rho_{NBO}$	-0.26	-0.26	0.13	0.12	0.10	0.09	-0.26	-0.26
µd/ debay	5.99	5.99	9.10	8.96	4.04	4.47	6.81	6.07
	C– a	**C – b**	**C– c**	**C– d**	**D-a**	**D-b**	**D-c**	**D-d**
E_{ads}	-36.22	-32.06	-28.06	-48.16	-39.53	-11.01	-28.34	-35.37
$E_{def\ NH2NO2}$	-0.46	-0.56	-0.36	-35.21	-115.99	0.83	-60.31	-60.44
$E_{def\ nano}$	-4.69	-0.43	-0.23	-169.25	-23.78	-3.58	-29.61	-31.31
$E_{def\ tot}$	-7.59	-0.98	-0.02	-204.32	-139.78	-4.41	-89.92	-91.75
E_{bin}	-43.82	-0.05	-0.04	-169.38	-177.31	-15.43	-3.58	-118.35
d	1.91	4.04	3.76	2.02	3.40	3.70	1.93	3.37
$\Delta\rho_{NBO}$	0.06	0.04	0.09	-0.55	0.05	0.06	-0.26	0.11
µd/ debay	4.65	7.60	4.11	6.81	4.05	4.48	6.08	8.35

Whereas the adsorption energy of N (NO_2) in **c** orientation for A−c, B−c, C−c and D−c models are −28.02, −14.03, −28.06 and −28.34 Kcal/mole respectively. It is notable that the calculated adsorption energy of NH_2NO_2 over Ni functionalize site of nanotube at the B−b, B−c and B−d models except B−a is much smaller than other sites. Thereby the adsorption of NH_2NO_2 molecule on Ni site of nanotube is not a favorable case. It seems that high value of adsorption energy at C−d model is not merely attributed to the strong nucleophilic property of N atom of NH_2 section. However, its high value of adsorption energy also is consequences of its neighboring functionals effects and adsorption of NH_2NO_2 molecule from H and N site when it is approached from N site of NH_2 section. On the other hand, in the B−d model due to dissociation of NH_2NO_2 on the surface of nanotube the adsorption energy is smaller than other models. In order to determine the amount of nanotube deformation, we have calculated the deformation energy of NH_2NO_2, GaNNTs, and NH_2NO_2/GaNNTs in NH_2NO_2/nanotube complex by using following equation:

$$E_{det-J} = E_{J-pure} - E_{J\ in\ GaNNTs/NH_2NO_2\ complex} \quad (2)$$

Here J is NH_2NO_2, GaNNTs, E_{J-pure} is total energy of NH_2NO_2, or GaNNTs in pure state, the $E_{J\ in\ GaNNTs/NH2NO2\ complex}$ is the total energy of J in complex when other compound is absent oneself.

$$E_{bin} = E_{GaNNTs/NH_2NO_2} - (E_{GaNNTs\ in\ complex} + E_{NH_2NO_2\ in\ complex}) \quad (3)$$

By using Eq. 3 we calculate the binding energy for adsorption NH_2NO_2 on the surface of nanotube, and the calculated results are listed in Table 1. As it can be seen from Table 1 the deformation energy values of NH_2NO_2, GaNNTs and NH_2NO_2/GaNNTs complex are negative and exothermic. The negative values of deformation energy indicate that the deformation process occur spontaneously at all models. It is worth mention that the deformation energy NH_2NO_2 molecule and GaNNTs in all adsorption systems are in range −0.36 to −115.99 and −0.23 to −169.25 Kcal/mol respectively.

On the basis of calculated results, when NH_2NO_2 molecule adsorb on the Ni site at the B−a, B−b, B−c and B−d models and N site at the C−a, C−b, C−c and C−d models the deformation energy of NH_2NO_2 molecule reduce significantly from pristine models. Hence, the deforming NH_2NO_2 molecule on the Ni site of Ni functionalized and N site of pristine GaNNTs is lower than other sites, whereas the deforming NH_2NO_2 molecule at Ga site of pristine GaNNTs is more than other site. The deformation energy GaNNTs in the C−a, C−b, and C−c models is much lower than other models, whereas the deformation energy of C−d models is more than other models. Comparison calculated results show that the binding energy of NH_2NO_2 on the surface of nanotube is in range −0.053 to −179.09 Kcal/mol. Overall, comparing the binding energies of system indicate that the binding of NH_2NO_2 molecule at the A−a (−170.06), A−d (−170.22), B−a(−179.09), C−d (−169.38) and B−a (−177.31) are more favorable than other those models. On the other hand, the binding energy of C−b and C−c models is lower and more unfavorable than than other models. This means that, the NH_2NO_2 approach to the N site of nanotube from O and N (NO_2) atoms prefer stay out of nanotube.

The recovery time of GaNNTs for adsorption of NH_2NO_2 at room temperature is computed according to the formula $\tau = \nu_0^{-1} e^{(-Eads/K_BT)}$, where T is temperature, K_B the Boltzmann's constant 0.00199 Kcal/mol. K and ν_0 is the attempt frequency (10^{-12} s^{-1}). The results of the strong adsorption between the NH_2NO_2 and the pristine and Ni functionalized GaNNTs suggest that, they are not remarkable in gas detection because such strong adsorptions imply that desorption of the adsorbate could be difficult and the device may suffer from long recovery times.

To investigate the thermodynamic feasibility of the NH_2NO_2 adsorption on the surface pristine and Ni functionalized GaNNTs several thermodynamic parameters such as the changes of internal energy (ΔE), enthalpy changes (ΔH), entropic changes (ΔS) and Gibbs free energy changes (ΔG) for all models at 298.14 K and 1 atm are calculated and the calculated results are given in Table 2.

Table 2. Thermodynamic parameters for adsorption NH_2NO_2 on the surface for A-a to D-d models (see Figs.1-4)

	ΔE Kcal/Mol	ΔH Kcal/Mol	ΔG Kcal/Mol)	ΔS Cal/Mol.K	ΔCV Cal/Mol.K
A-a	-41.85	-36.17	-23.36	-42.96	4.74
A-b	-12.84	-13.43	-1.21	-40.99	6.44
A-c	-27.53	-28.12	-12.83	-51.28	4.65
A-d	-28.54	-36.16	-22.36	-46.29	9.26
B-a	-42.84	-36.17	-23.36	-42.96	4.74
B-b	-13.84	-13.43	-1.21	-40.99	6.44
B-c	-26.53	-28.12	-12.83	-51.28	4.65
B-d	-29.54	-36.16	-22.36	-46.29	4.74
C-a	-30.30	-54.12	-39.67	-48.47	5.59
C-b	-34.66	-26.49	-15.56	-36.66	3.93
C-c	-25.75	-26.35	-15.84	-35.25	4.17
C-d	-47.17	-47.77	-33.48	-47.93	4.61
D-a	-37.18	-37.77	-24.54	-44.37	4.85
D-b	-27.88	-19.15	-5.68	-45.18	4.75
D-c	-10.34	-28.47	-12.66	-53.03	6.50
D-d	-37.99	-35.58	-21.99	-45.58	4.69

Comparison thermodynamic results show that the ΔE and ΔH values of the A−a to D−d models are in range −10.34 to −47.17 Kcal/mol and −13.43 to −47.77 Kcal/mol respectively, the negative values of ΔE and ΔH reveal that the adsorption of NH_2NO_2 molecule on the surface of pristine and Ni functionalized GaNNTs is exothermic. In the A, B, C and D model when the NH_2NO_2 molecule adsorb from H (NH2) site of NH_2NO_2 the values of the ΔE and ΔH are more negative than other site of NH_2NO_2 molecule and this lead to strong interaction between nanotube and nitramine compound.

However, the ΔG and ΔS values for the A−a to D−d are in range −1.21 to −39.67 Kcal/mol and −35.25 to −53.03 Kcal/mol respectively. The negative values of ΔE reveal that the adsorption of NH_2NO_2 molecule on the surface of GaNNTs is stable in thermodynamic approach and it can happen spontaneously at room temperature and 1 atm.

It is clearly observed that in the A−a, B−a, C−a, and D−a with more changes in Gibbs free energy and enthalpy are thermodynamically feasible and the NH_2NO_2 molecule prefers to be adsorbed from H site (NH_2) on the surface of nanotube. Whereas, in the A−b, B−b, C−b and D−b with low changes in Gibbs free energy and enthalpy are thermodynamically unfavorable and the adsorption of NH_2NO_2 molecule from O site (NO_2) on the surface nanotube is weaker than other site.

Overall, Comparison the changes of Gibbs free energy and enthalpy for the A−a, B−a, C−a, D−a, A−b, B−b, C−b, and D−b models are shown in Fig 4. It is seen that the adsorption NH_2NO_2 molecule from H site (NH_2) on the N site of the pristine GaNNTs (C−a model) is more favorable, stable and spontaneous than other those models in thermodynamic approach.

A comparing of the ΔH and ΔG parameters clearly indicates the values of ΔH are larger than ΔG values due to the entropic effect. The entropic values of all adsorption models are negative and this result confirms that the adsorption of NH_2NO_2 on the surface of nanotube is unflavored in entropical approach. The thermal specific coefficient changes of all adsorption models are positive and are in range 3.93 to 9.26 Kcal/mol.

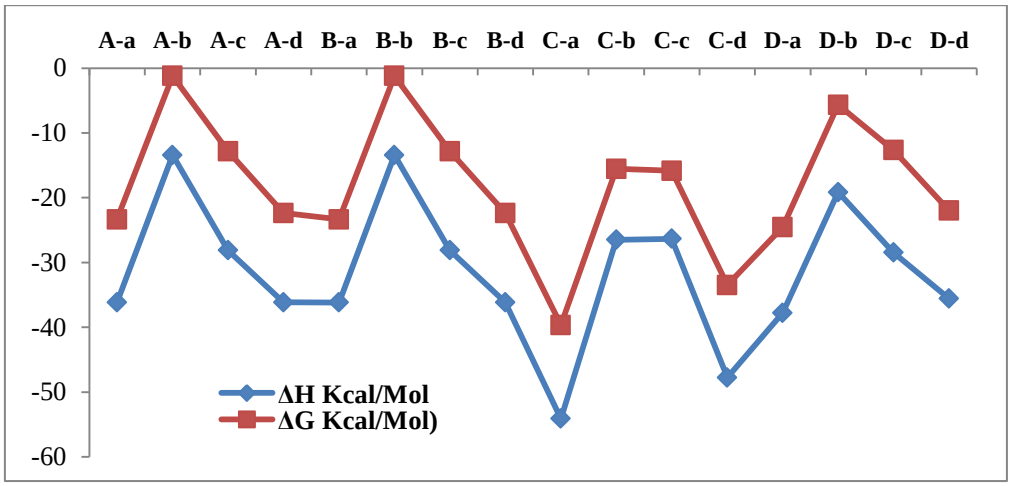

Fig. 4. Diagram of thermodynamic parameters for A−a to D−d adsorption models (see Fig. 2).

3–2 HOMO–LUMO and quantum descriptors analysis

In order to reach deeper understanding about the adsorption of NH_2NO_2 molecule on the electronic properties of pristine and Ni functionalized GaNNTs the distribution of densities and their energies of the HOMO and LUMO of all the A−a to D−d models are calculated and the results are shown in Fig. 5 and are tabulated in Table 3. Comparison results reveal that at the A−a, A−b, A−c, A−d, C−a, C−b, C−c, and C−d models the HOMO orbital densities are distributed uniformly around nanotube. Whereas at the B−a, B−b, B−c, B−d, D−a, D−b, D−c and D−d models the HOMO orbital densities is mostly localized around Ni functionalized position. The HOMO energy of all adsorption models is in range −7.66 to −6.28 eV and the LUMO energy is in range −2.75 to −0.22 eV. Comparison results reveal that the HOMO energy of A and B models is lower than C and D models due to Ni functionalized. Whereas the LUMO energy of B−c (−0.22 eV), B−a (−0.34 eV), A−a (−0.34 eV), B−d (−0.48 eV) and D−c (−0.71 eV) is strongly more than other those adsorption models. In these models when NH_2NO_2 adsorb on the surface of nanotube the level energy of unoccupied orbital increase significantly from original values. Whereas the level of HOMO energy change slightly from original values or almost unchanged. This result can be confirm that the adsorption NH_2NO_2 molecule has acceptor electron effect and decrease the charge density around nanotube. The positive values of the maximum amount of electronic charge (ΔN) indicate that charge transfer occur from NH_2NO_2 molecule toward nanotube. On the other hand, for investigating the effect of NH_2NO_2 on the electrical properties of nanotube we calculate the gap energy between HOMO and LUMO energy ($E_{gap}=E_{LUMO}-E_{HOMO}$). Based on calculated results in Table 3, it can see the gap energy of all adsorption models are in range 4.00 to 7.32 eV. The biggest gap energy is 7.32 eV for the A−b and B−a, and the lowest gap energy is 4.00 eV for D−b model. Thereby the conductivity and activity of D−b model is more than other models whereas these properties for A−b and B−a models are lower than other those models. The order of decrement in gap energies of A, B, C and D models in the a, b, c and d direction are: A−a=B−a> D−a> C−a, B−b>A−b> C−b> D−b, B−c> D−c>A−c> C−c and B−d> A−d> D−d> C−d.

These comparisons of gap energy indicate that in the all adsorption models the changes in gap energy directly is dependent to the orientation of NH_2NO_2 adsorption on the surface of nanotube. The percent changes of gap energy are determined by Eq. 4:

$$\%\Delta E_{gap}=\frac{(E_{g\,nano/NH_2NO_2}-E_{g\,nano})}{E_{g\,nano}}\times 100 \qquad (4)$$

According to calculated results of Table 3, it is clearly observed that the $\%\Delta E_{gap}$ values for all adsorption models except D−a, D−c and D−d models are negative, the negative values of $\%\Delta E_{gap}$ expresses that the gap energy of nanotube decrease from original values due to NH_2NO_2 adsorption effects, resulting the conductivity of nanotube increase.

Comparison results indicate that the most decrement in gap energy is exhibited in the A−c (38.83%), A−b (36.92%), B−b (33.24) and D−b (32.20%) models, whereas the lowest decrement in gap energy is shown in the A−a (0.27%), B−a (0.27%) and B−c(0.68%). On the other hand, in the D−a, D−c, and D−d models the $\%\Delta E_{gap}$ values are positive and show that the gap energy of these models increase slightly from original state.

To better understanding, the electronic properties of NH_2NO_2 adsorbed on the

surface of pristine Ni functionalized GaNNTs; we calculate the total density of states (DOS) for all adsorption models in range −15 to 10 eV and results are presented in Fig. 6.

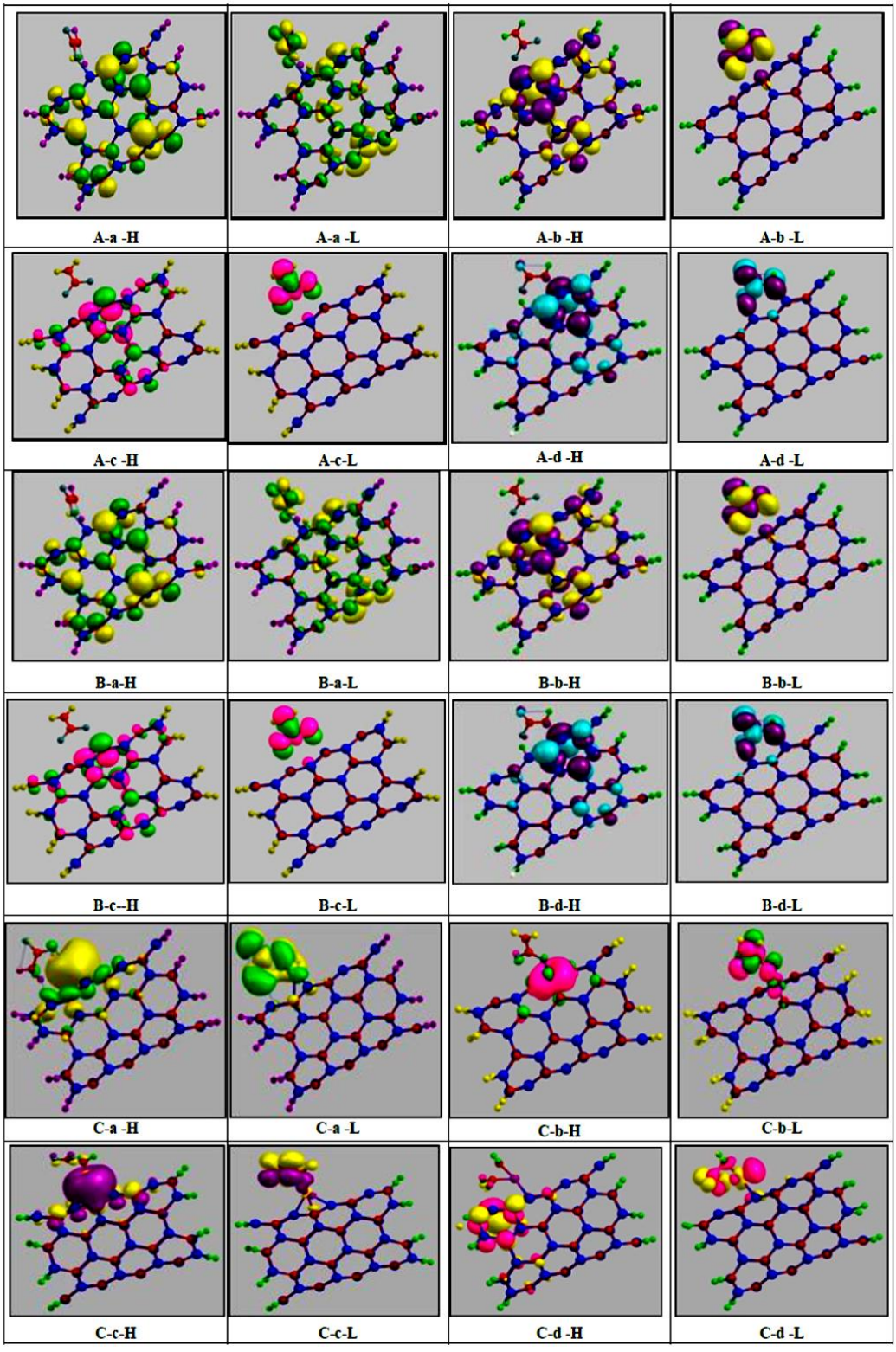

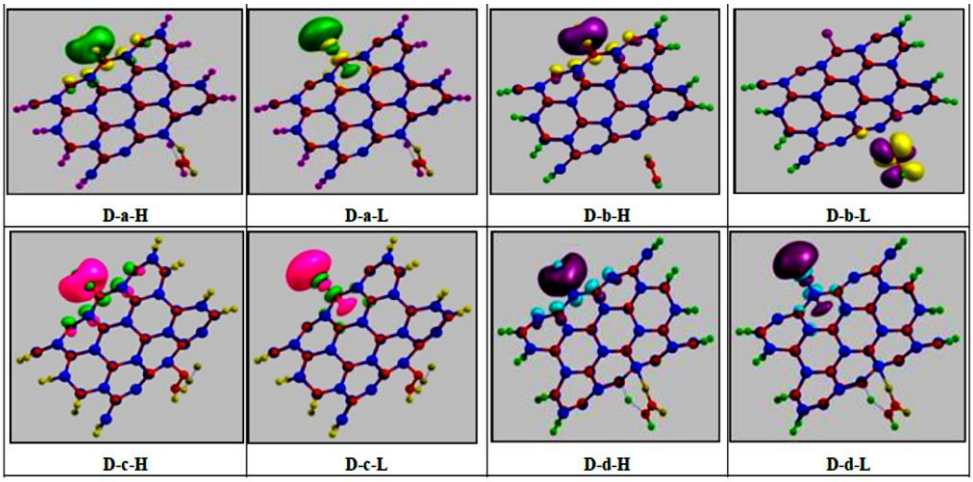

Fig. 5. Plots of HOMO and LUMO energy structures for A−a to D−d adsorption models (see Fig. 2).

Table 3. Calculated quantum parameters for adsorption NH_2NO_2 on the surface for A-a to D-d models (see Figs. 1-4)

property	A-a	A-b	A-c	A-d	B-a	B-b	B-c	B-d
E_{HOMO}	-7.66	-7.26	-7.24	-7.39	-7.66	-7.24	-7.51	-7.55
E_{LUMO}	-0.34	-2.63	-2.75	-1.09	-0.34	-2.34	-0.22	-0.48
ΔE_{gap}	7.32	4.63	4.49	6.30	7.32	4.90	7.29	7.07
I (ev)	7.66	7.26	7.24	7.39	7.66	7.24	7.51	7.55
A (ev)	0.34	2.63	2.75	1.09	0.34	2.34	0.22	0.48
μ (ev)	-3.99	-4.95	-5.00	-4.24	-3.99	-4.79	-3.86	-4.02
χ (ev)	3.99	4.95	5.00	4.24	3.99	4.79	3.86	4.02
η (ev)	3.66	4.63	2.24	3.15	3.66	2.45	3.65	3.54
S (ev)$^{-1}$	0.14	0.22	0.22	0.16	0.14	0.20	0.14	0.14
E_{FL}(ev)	-3.99	-4.95	-5.00	-4.24	-3.99	-4.79	-3.86	-4.02
$\Delta\varphi$ (ev)	-3.67	-2.32	-2.24	-3.15	-3.66	-2.45	-3.65	-3.54
ΔN (ev)	1.10	2.13	2.23	1.35	1.09	1.95	1.10	1.13
ω (ev)	2.18	5.28	5.57	2.90	2.18	2.90	2.04	2.28
$\%\Delta E_{gap}$	-0.27	-36.92	-38.83	-14.17	-0.27	-33.24	-0.68	-3.68
	C-a	C-b	C-c	C-d	D-a	D-b	D-c	D-d
E_{HOMO}	-6.38	6.28-	-6.68	-7.25	-6.73	-6.42	-6.62	-6.73
E_{LUMO}	-1.45	1.82-	-2.20	-1.84	-0.80	-2.42	-0.71	-0.82
ΔE_{gap}	4.93	4.46	4.48	5.41	5.92	4.00	5.91	5.91
I (ev)	6.38	6.28	6.68	7.25	6.73	6.42	6.62	6.73
A (ev)	1.45	1.82	2.20	1.84	0.8	2.42	0.71	0.82
μ (ev)	-3.92	4.04-	-4.44	-4.54	-3.77	-4.42	-3.66	-3.77
χ (ev)	3.92	4.04	4.44	4.54	3.77	4.42	3.66	3.77
η (ev)	2.46	2.23	2.24	2.70	2.96	1.99	2.95	2.95
S (ev)$^{-1}$	0.20	0.22	0.22	0.18	0.17	0.25	0.17	0.17
E_{FL}(ev)	-3.92	-4.05	4.44-	-4.54	-3.77	-4.42	-3.65	-3.77
$\Delta\varphi$ (ev)	-2.46	-2.23	-2.24	-2.71	-2.96	-2.00	-2.97	-2.96
ΔN (ev)	1.59	1.81	1.98	1.68	1.27	2.21	1.24	1.28
ω (ev)	3.11	3.67	4.40	3.82	2.40	4.89	2.26	2.26
$\%\Delta E_{gap}$	-16	-24	-24	-8	0.34	-32	0.17	0.17

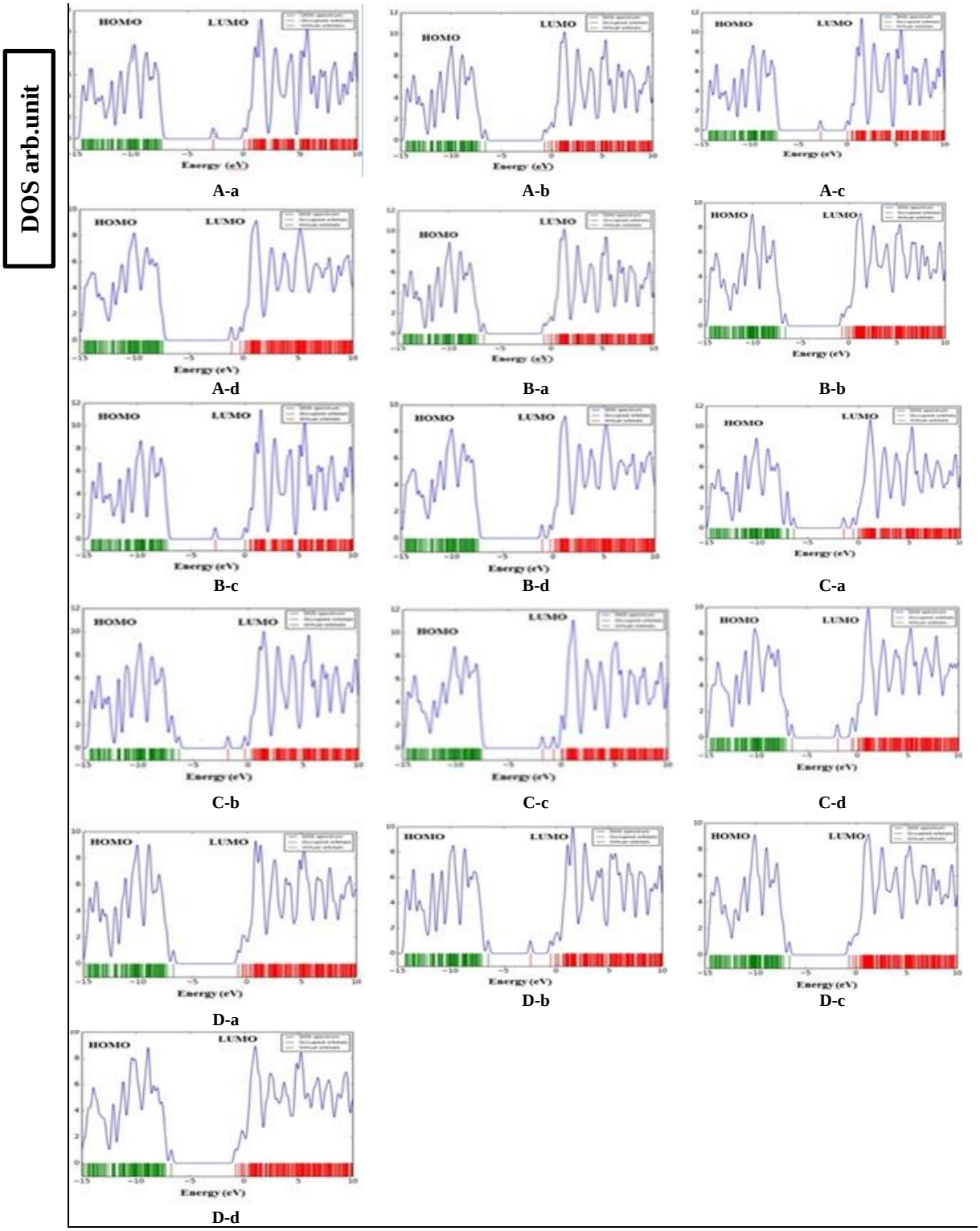

Fig. 6. DOS Plots for adsorption for A−a to D−d adsorption models (see Fig. 2).

It can be observed that in the A, B, C and D models, in the occupied orbitals region and virtual orbital region there is 8 and 10 maximum peaks respectively. It is notable that by adsorbing the NH_2NO_2 molecule on the B−c and D−b models due to appearing one peak in the gap region the E_{gap} decreases significantly from original

values. The global hardness (η) and global softness (S) of all adsorption models are calculated by using Eqs. 5 and 6 and the calculated results are listed in Table 3.

$$\eta = 1/2(E_{LUMO} - E_{HOMO}) \quad (5)$$

$$S = 1/2\eta \quad (6)$$

It is known that the global hardness is a parameter that is applied to represent the resistance towards the deformation of electron cloud of chemical systems under small perturbation encountered during the chemical process. Comparison results display that the global hardness values of all adsorption models is in range 1.99 to 4.63 eV and with functionalizing Ni atom the global hardness of NH_2NO_2/Nanotube complex decrease significantly from pristine models. Therefore, Ni functionalized reduces the resistance of electron cloud deformation of system and so the activity of system enhance from pristine models. The most enhancements in the activity of system are occurred in the D−b model.

The chemical potential (μ) and electronagivity of nanosheet (χ), index of electrophilicity (ω) and charge transfer parameters (ΔN) of the all adsorption models are calculated by using Eqs 7−10 [34−35].

$$\mu = (E_{HOMO} + E_{LUMO})/2 \quad (7)$$

$$\chi = -\mu \quad (8)$$

$$\omega = \mu^2/2\eta \quad (9)$$

$$\Delta N = (-\mu/\eta) \quad (10)$$

It is shown that the chemical potential of all adsorption models are negative in range −3.66 to −5.00 eV and it means that all adsorption systems are stable and do not decompose spontaneously into the particles they are made up. The chemical potential of pristine and Ni functionalized GaNNTs is −3.89 and −3.65 eV respectively. With adsorbing NH_2NO_2 molecule except B−c model the chemical potential values of all models are more negative than original values, and all adsorption models are more stable than original state, this result confirms that the pristine and Ni functionalized GaNNTs can be a good candidate to adsorbing NH_2NO_2.

The electronagivity of nanosheet (χ), index of electrophilicity (ω) and charge transfer parameters (ΔN) of all adsorption models are in range 3.66 to 5.00 eV, 2.18 to 5.57 eV and 1.09 to 2.23 eV. The work functions ($\Delta\varphi$) of all adsorption system is calculated by Eq. 11

$$\Delta\varphi = E_{HOMO} - E_{FL} \quad (11)$$

The work function is the least amount of energy required to remove an electron from the Fermi level to far from system. The change of work function of nanotube after the NH_2NO_2 adsorption alters its field emission properties. The emitted electron current densities in a vacuum are theoretically calculated by $j = AT^2 \exp^{(-\Delta\varphi/kT)}$, here A is called the Richardson constant (A/m^2), T is the temperature (K). Based on calculated results of Table 3, the work function of the system is in range −2.00 to −3.67 eV. The calculated results indicate that the work function of Ni functionalized models is more than pristine models, and with adsorbing NH_2NO_2 molecule in the A−b, A−c, B−b, C−a, C−b, C−c, and D−b models the work function parameter increase significantly from original values. According to Richardson function, the emitted electron current densities (j) values decrease significantly from original values. These results confirm that the adsorbing NH_2NO_2 molecule change the optical properties of system.

3.3 Atom in molecule (AIM) analyses

Here, we use the atom in the molecule theory to determine the nature of the

NH_2NO_2 interaction with the pristine and Ni functionalized GaNNTs. For this aims at the relevant topological results such as bond critical point (BCP) the electron densities (ρ), the total electronic energy (H_{BCP}), the potential energy (V_{BCP}) and the kinetic energy (G_{BCP}) and Laplacian of electron densities ($\nabla^2\rho$) are calculated by using AIMALL program [37].

These parameters closely relate to the type and strength of the interactions between the attractive atom pairs. The topological properties of ρ_{BCP}, $\nabla^2\rho$, H_{BCP}, V_{BCP}, and G_{BCP} for the B−a, B−b, B−d, C−a, C−b, C−c, C−d, D−a, D−b, D−c and D−d due to interaction NH_2NO_2 with pristine and Ni functionalized GaNNTs are listed in Table 4.

The values of $\rho_{BCP,}$ $\nabla^2\rho$, H_{BCP} and V_{BCP}, for the B−d, D−a, and D−d are positive and significantly larger than those other adsorption models. These results indicate that the covalent bonding interactions between NH_2NO_2 and nanotube are stronger than those other models. The positive values of all $\nabla^2\rho$ confirm the noncovalent nature of these interactions. With respect to the sign of Laplacian of electron density on BCPs data, existence of electrostatic type of interactions, which is a subset of noncovalent interactions, would be proved. The $\nabla^2\rho > 0$ implies that the interaction is dominated by the contraction of ρ_{BCP} towards each nucleus. On the other models, the $\nabla^2\rho < 0$ indicates the concentration of charge towards interaction line. The concentration of charge leads to contraction of ρ perpendicular to the interaction line and lowers the potential energy. The magnitude of lowering of the potential energy is greater than the kinetic energy from the same region thereby creating attractive force and bound shared interaction.

3.4 Molecular electrostatic potential

Molecular electrostatic potential (MEP) is one of the important method that is used to give information about the net electrostatic effect produced at that point by total charge distribution (electron + proton) of the molecule and correlates with dipole moments, electronegativity, partial charges and chemical reactivity of the molecules. It provides a visual method to understand the relative polarity of the molecule. An electron density isosurface mapped with electrostatic potential surface depicts the size, shape, charge density, and site of chemical reactivity of the molecules [38−39]. The ESP plots of all adsorption models are given in Fig. 7. In these plots, the red color represents the negative charges or the electrophilic regions and the blue color represents the positive charges or the nucleophilic regions.

Table 4. Calculated AIM parameters for adsorption NH_2NO_2 on the surface for A-a to D-d models (see Fig. 1)

	bond	$\rho_{BCP(a.u.)}$	$\nabla^2\rho_{BCP(a.u.)}$	$H_{BCP(a.u.)}$	$G_{BCP(a.u.)}$	$V_{BCP(a.u.)}$	|Gc/Vc|
B-a	**H-N**	0.091	-0.090	0.110	0.110	0.382	0.150-
B-b	**O-N**	0.072	-0.021	0.034	0.034	0.041	0.780
B-d	**H-N**	0.290	0.302	0.051	0.052	0.410	0.131
C-a	**O-Ni**	0.042	0.031-	0.010	0.024	0.030	0.131
C-b	**O-Ni**	0.121	0.132-	0.042	0.173	0.211	0.510
C-c	**Ni-N**	0.120	0.122-	0.043	0.172	0.210	1.590
C-d	**Ni-N**	0.110	0.121-	0.031	0.141	0.181	0.130
D-a	**H-N**	0.273	0.281	0.330	0.051	0.380	0.131
D-b	**O-N**	0.007	0.001-	0.003	0.003	0.005	0.511
D-c	**N-N**	0.012	0.006-	0.012	0.020	0.031	1.590
D-d	**H-N**	0.270	0.280	0.370	0.321	0.051	0.130

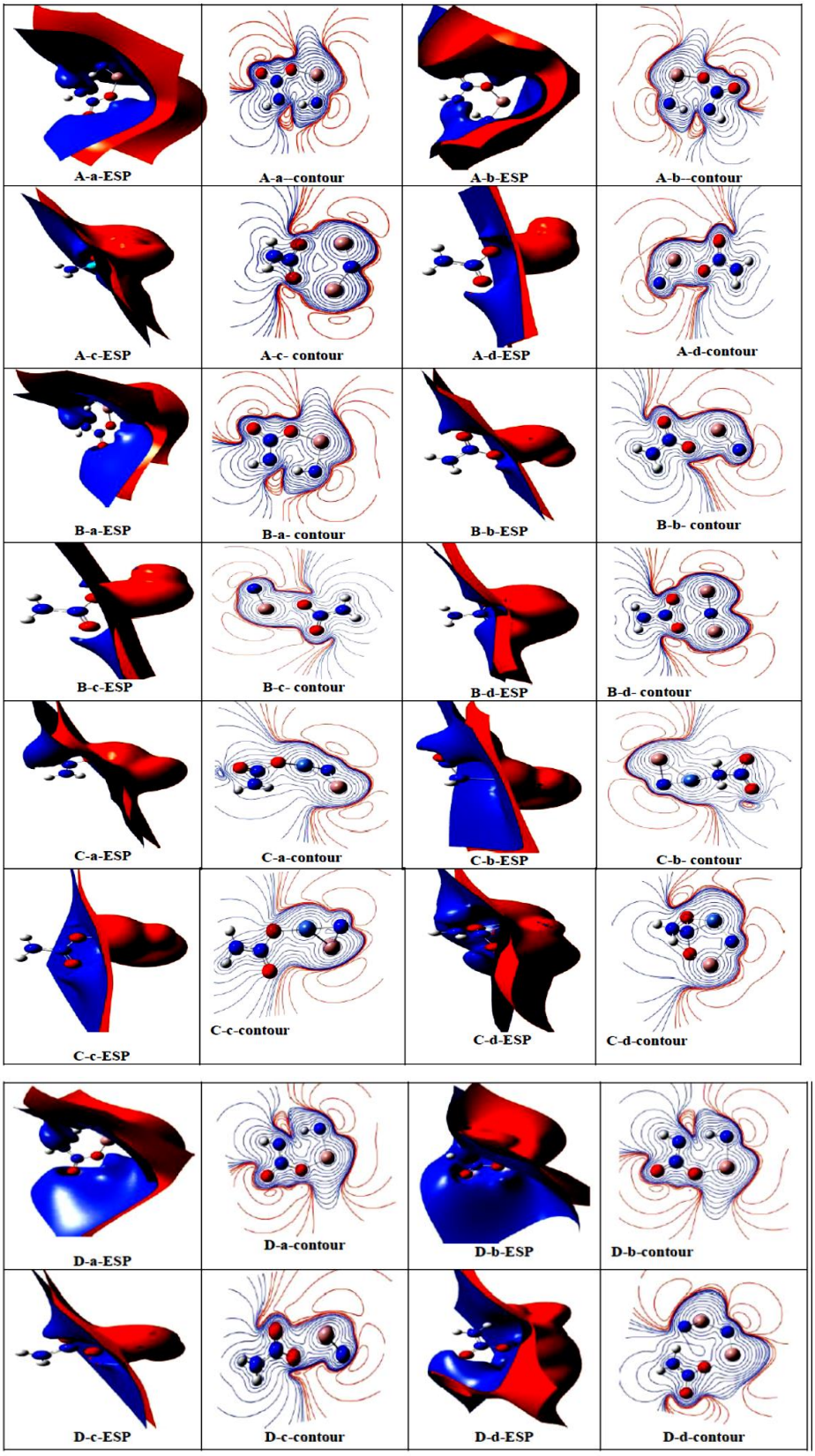

Fig. 7. The MEP Plots for A−a to D−d adsorption models (see Fig. 2).

Based on the calculated results in Fig. 7, the most electron density, and negative potential, red color, is distributed around nanotube adsorption position and the most positive potential, blue color, is localized around NH_2NO_2 molecule. This result indicates that a low charge transfer from the NH_2NO_2 molecule toward the nanotube ones resulting in a weak ionic bonding in the GaNNTs/NH_2NO_2 complex. This result confirms that after adsorbing NH_2NO_2 molecule the exterior surface of nanotube is rich of electron charge and the NH_2NO_2 surface is poor of charge electron. The contour map of all models show that the layers of red color strongly overlap on around adsorbent compound and the blue color layers strongly overlap on far from adsorption position.

3.5. NBO analyses

A natural bond orbital (NBO) analysis is one another important parameters to gain more details about interaction between NH_2NO_2 as adsorbate and pristine, Ni functionalized GaNNTs as adsorbent. The results indicate that NH_2NO_2 molecule is a NBO donor and the GaNNTs apply as NBO acceptor. From NBO results, the second−order perturbation interaction energy $E^{(2)}$ [40−41] between each donor NBO and acceptor NBO, delocalization $i \rightarrow j$ is calculated. The selected donor and acceptor orbitals are displayed in Fig. 8.

According to the calculated NBO results the transition electron from the donor to acceptor orbitals: the $\sigma_{N\,41-Ga\,47} \rightarrow \sigma^*_{Ga\,44-N\,41}$ for A models (I), $\sigma_{N\,46-Ga\,47} \rightarrow \sigma^*_{Ga\,45-N\,46}$ for B models (J), $\sigma_{N\,41-Ga\,44} \rightarrow \sigma^*_{Ga\,51-N\,52}$ for C model (K) and $\sigma_{N\,43-Ga\,42} \rightarrow \sigma^*_{Ga\,42-N\,43}$ for D models (L) have more $E^{(2)}$ values (see Fig. 8). Comparison results reveal that in the A, B, C and D models the transition donor to acceptor orbital I, J, K and L is in range 1.49 to 2.84 kcal/mol. It is notable that the $E^{(2)}$ values is dependent to direction of NH_2NO_2 molecule adsorption. In the A and B models the $E^{(2)}$ values is in order: b> c> a> d and in the C model is in order d> a> b=c and for D model is in order: d> c> b> a. These results lead to Ni−functionalized GaNNTs having higher polarizability than NH_2NO_2 molecule, and so the NH_2NO_2 adsorption changes significantly the electrical properties of nanotube from original state. Moreover, the greatest stabilization energy for Ni−functionalized complex is accordance with the shortest interaction distance. The $\Delta\rho_{(NBO)}$ charge

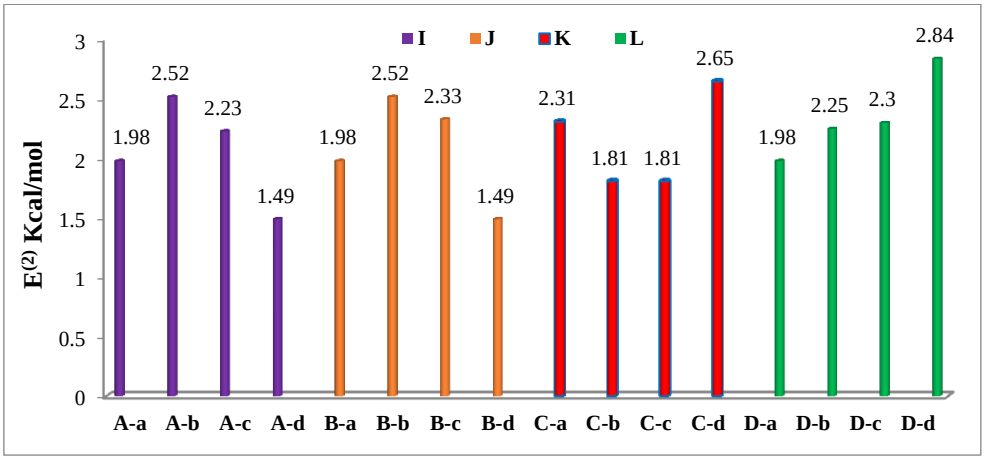

Fig. 8. The stabilization energy $E^{(2)}$ Plots for for A−a to D−d adsorption models (see Fig. 2).

density on the surface NH_2NO_2 molecule is in range of −0.26 |*e*| to +0.13 |*e*| (see Table 1). The positive values of the $\Delta\rho_{(NBO)}$ values for all adsorption models except the A−a, A−b, B−c, B−d, C−d and D−c models confirm that the NH_2NO_2 in these process act as electron donor, and these results are in agreement with the positive values of maximum amount of electronic charge (ΔN) transfer and HOMO−LUMO results.

4. CONCLUSIONS

In the current work, the effects of NH_2NO_2 adsorption on the pristine and Ni functionalized GaNNTs by using DFT method at cam−B3LYP/6−31G (d) level of theory.

The adsorption energy of all adsorption models is negative and exothermic in view of thermodynamic approach. The calculated results reveal that the adsorption energy of NH_2NO_2 on the Ni functionalized site of nanotube at the B−b, B−c, and B−d models except B−a is much smaller than other sites. The ΔG and ΔS values for the A−a to D−d are in range −1.21 to −39.67 Kcal/mol and −35.25 to −53.03 Kcal/mol respectively. It is worth mention that the deformation energy of NH_2NO_2 molecule and GaNNTs in all adsorption systems is in range −0.36 to −115.99 and −0.23 to −169.25 Kcal/mol respectively. On the other hand, the deforming NH_2NO_2 molecule on the Ni site and N site of pristine GaNNTs is lower than other sites. From HOMO−LUMO energy, it is found that the biggest gap energy is 7.32 eV for A−b and B−a, and the lowest gap energy is 4.00 eV for D−b model. The calculated results demonstrate that with functionalizing Ni atom the global harness of NH_2NO_2/nanotube complex decrease significantly from pristine models and so the activity of complex increase significantly from original state. The calculated results reveal that with adsorbing NH_2NO_2 molecule in the A−b, A−c, B−b, C−a, C−b, C−c, and D−b models the work function parameter increase significantly from original values.

ACKNOWLEDGMENT

The author thanks the Computational information center of Malayer University for providing the necessary facilities to carry out the research.

SUPPLEMENTARY DATA

Tables S1− S8 and Figures S1− S3 are given in supplementary data.

REFERENCES

[1] H. P. Li, N. Q. Zhao, C. N. He, C. S. Shi, X. W. Du, J. J. Li, J. Alloys Comp.465 (2008) 51-55

[2] A. A. Zouhbi, N. S. Al−Din, Opt. Rev. 15(2008) 251-254

[3] Y. Al−Douri Y., Proc. Eng. 53 (2013) 400-404

[4] G. X. Chen, Y. Zhang, D. D. Wang, J. M. Zhang, K. W. Xu, Solid State Commun. 151(2011) 139-143

[5] S. Hao, G. Zhou, J. Wu, W. Duan, B. L. Gu, Chem. Phys. Lett. 401(2005)47-51

[6] A. Mohanbabu, N. Anbuselvan, N. Mohankumar, D. Godwinraj, C. K. Sarkar, Solid−State Electron. 91(2014) 44-52

[7] S.C. Hung, Y.K. Su, S.J. Chen, L.W. Ji, T.H. Fang, L.W.Tu, M. Chen, Appl. Phys. A 80 (2005)1607-1610

[8] C. Hemmingsson, G. Pozina, S. Khromov, B. Monemar, Nanotechnology. 22 (2011) 085602.

[9] Y.S. Park, G. Lee, M.J. Holmes, C.C.S. Chan, B.P.L. Reid, J.A. Alexander−Webber, R.J. Nicholas, R.A. Taylor, K.S. Kim, S.W. Han, W. Yang, Y. Jo,J. Kim, H. Im, Nano Lett. 15 (2015) 4472−4476.

[10] Z. Wang, G.Q. Yin, L. Jing, J. Shi, Z. Li, Int. J. Mod. Phys. B 28 (2014).
[11] [11] E. Li, X. Wang, L. Hou, D. Zhao, Y. Dai, X. Wang, J. Phys. Conf. Ser. 276 (2011) 012046-5.
[12] V. Chakrapani, ECS Trans. 66 (7) (2015) 29−37.
[13] S. Hao, G. Zhou, W. Duan, J. Wu, B. L. Gu, J. Chem. Phys. 125 (17) (2006) 174711.
[14] D. Kumar, V. Verma, K. Dharamvir, H. S. J. Comput. Theor. Nanosci. 12 (3) (2015) 516−523.
[15] C. Li, S. Liu, A. Hurtado, J. B. Wright, H. Xu, T. S. Luk, J. J. Figiel, I. Brener, S. R. J. Brueck, G. T. Wang, ACS Photonics 2 (2015) 1025−1029.
[16] T. W. Lin, S. Y. Choi, Y. H. Kim, M. L. H. Green, Carbon 48 (2010) 2401−2408.
[17] M. Rezaei‑Sameti, F. Moradi, J. Incl. Phen. Macrocyclic Chem. 88 (2017) 209–218
[18] Q. Peng, C. Liang, W. Ji, S. De, Appl. Phys. A Mater. Sci. Process. 113 (2013) 483−490.
[19] H. Sahin, S. Cahangirov, M. Topsakal, E. Bekaroglu, E. Akturk, R. T. Senger, S. Ciraci, Phys. Rev. B 80 (2009)155453.
[20] J. V. N. Sarma, R. Chowdhury, R. Jayaganthan, Comput. Mater. Sci. 75 (2013)29−34.
[21] A. Shokri, F. Ghorbani Avaresi, Opt. Commun. 304 (2013)143−147.
[22] H. Yan, S. Liu, Z. Y. Gan, X. H. Song, J. P. Xu, Nanotechnol. Precis. Eng. 7 (2009)191−194.
[23] J. Zhang, S. A. Meguid, Nano Energy 12 (2015) 322−330.
[24] G. I. Giannopoulos, S. K. Georgantzinos, Eur. J. Mech. A Solids 65 (2017) 223−232
[25] S. Hassan Saberi, S. Mahdy Baizaee, H. Kahnouji, Superlat. Microstr. 74 (2014) 52–60
[26] J. M. Sodr, E. Longo, C. A. Taft, J. B.L. Martins, J. D. S .Santos, C. R. Chimie 20 (2017) 190−196
[27] A. Seif, T. S. Ahmadi, Cent. Eur. J. Chem. 8(4) (2010)913–918
[28] J. Liu, W. Jiang, Q. Yang, J. Song, G. Hao, F. Li, Def. Technol., 10 (2014) 184−189.
[29] J. Liu, W. Jiang, F. Li, Propellants Explos. Pyrotech. 39 (2014) 30−39.
[30] [30] M. Nayebzadeh, A. Ahmadi Peyghan, H. Soleymanabadi, Physica E 62 (2014) 48–54.
[31] J.Y. Zhao, F.Q. Zhao, X.H. Ju, H.X. Gao, S.Q. Zhou, J. Clust. Sci. 23 (2012) 395-410.
[32] S. Q. Zhou, F. Q. Zhao, X. H. Ju, X. C. Cheng, and J. H. Yi, J. Phys. Chem. C 114(2010) 9390-9397.
[33] J. Y. Zhao, F. Q. Zhao, X. H. Ju, H. X. Gao, S. Q. Zhou, J. Clust. Sci. 23(2012)395–410
[34] M. Rezaei−Sameti, N. Javadi Jukar, J. Nanostruct. Chem. 7(2017) 293–307.
[35] M. Rezaei−Sameti, M. Bagheri, J. Phys. Theo. Chem.14 (2017) 63-80.
[36] M. W. Schmidt, K. K. Baldridge, J. A. Boatz, S. T. Elbert, M. S. Gordon, J. H. Jensen, S. Koseki , N. Matsunaga, K. A. Nguyen, S. J. Su, T. L. Windus, M. Dupuis, J. A. J. Comp. Chem. 14 (1993) 1347-1363
[37] R. F. W. Bader, Atoms in Molecules: A Quantum Theory. Oxford University Press, New York. (1990).
[38] Z. Peralta−Inga, P. Lane, J. S. Murray, S. Boyd, M. E. Grice, C. J. O'Connor, P. Politzer, Nano. Lett. 3(1) (2003) 21−28.
[39] F. Bulat, A. Toro−Labbe, T. Brinck, J. S. Murray, P. Politzer, J. Mol. Mod. 16(11) (2010)1679−1691 (2010).

[40] L. J. Na, C. Z. Rang, Y. S. Fang, J. Zhejiang, Univ. Sci. 6 (2005)584-589.

[41] G. Keresztury, S. Holly, J. Varga, G. Besenyei, A. V. Wang, J. R. Durig, Spectrochim. Acta 49A (1993) 2007-2.17.